Probing Charged Lepton Flavor Violation at the EIC

Sonny Mantry
University of North Georgia

The 17th Annual Workshop on Tau Lepton Physics (TAU2023)
University of Louisville
December 5th, 2023

Lepton Flavor Violation

- Discovery of neutrino oscillations indicate that neutrinos have mass!
- Neutrino oscillations imply Lepton Flavor Violation (LFV).
- LFV in the neutrinos also implies Charged Lepton Flavor Violation (CLFV):

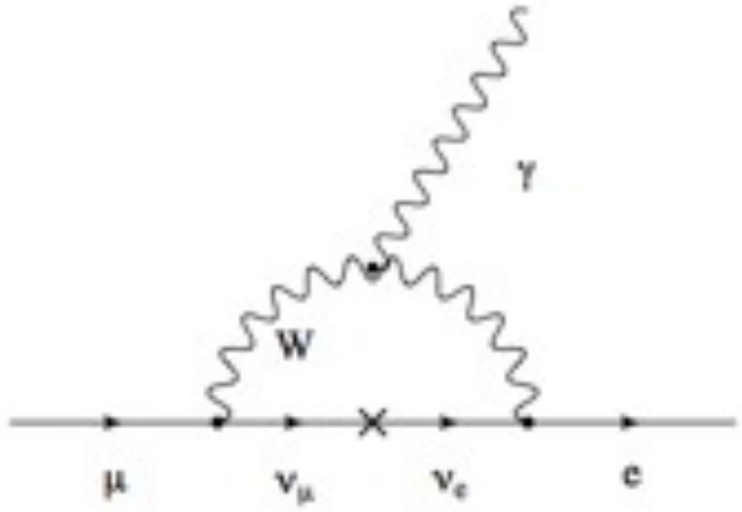

$$\mathrm{BR}(\mu \to e\gamma) < 10^{-54}$$

However, SM rate for CLFV is tiny due to small neutrino masses

- No hope of detecting such small rates for CLFV at any present or future planned experiments!

Lepton Flavor Violation in BSM

- However, many BSM scenarios predict enhanced CLFV rates:
  - SUSY (RPV)
  - SU(5), SO(10) GUTS
  - Left-Right symmetric models
  - Randall-Sundrum Models
  - LeptoQuarks
  - ...

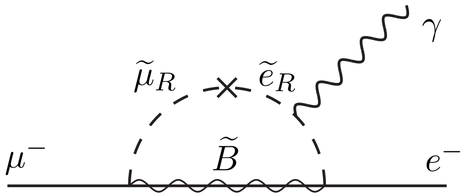

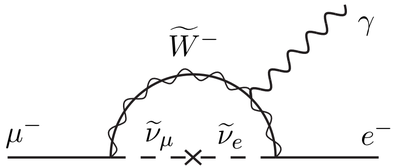

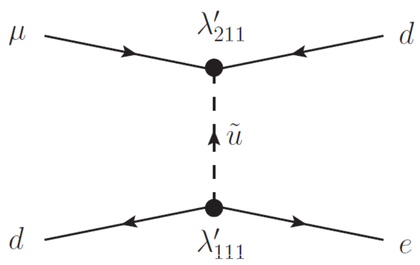

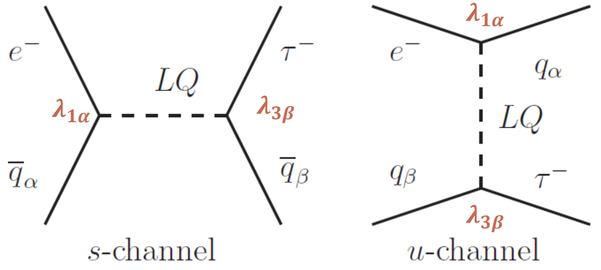

- Leptoquarks can generate CLFV at tree level! Likely to produce enhanced CLFV rates compared to loop level processes in other models.

Snowmass 2021 White Paper

[2203.14919 Banergee et. al.]

- Snowmass 2021 White paper provided a broad overview of the CLFV program.
- CLFV will be probed in a wide variety of experiments across the energy spectrum:

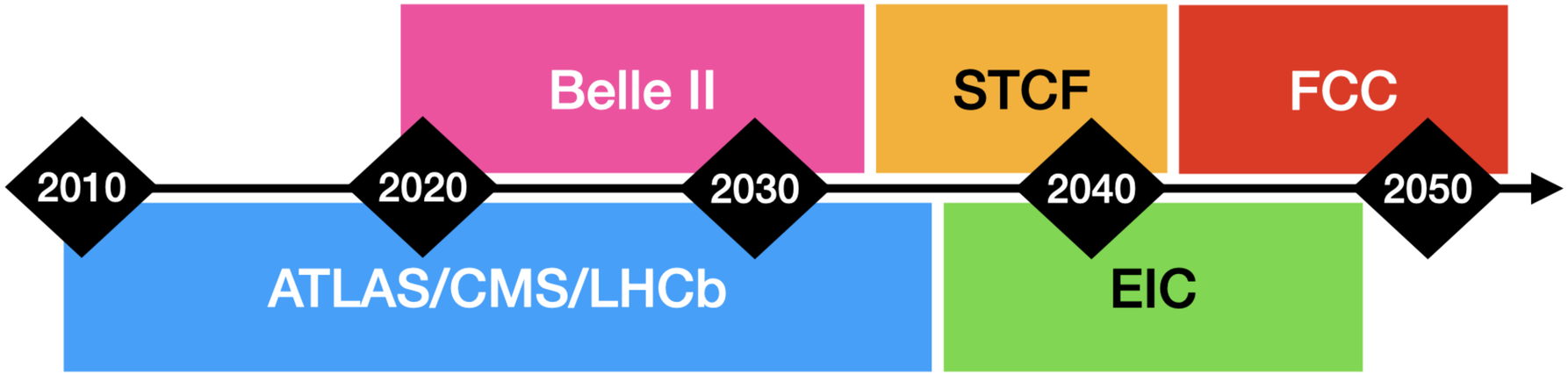

Figure 1: Tentative timeline for data-taking at different experiments probing CLFV in the τ sector.

Snowmass 2021 White Paper

[2203.14919 Banergee et. al.]

- CLFV will be searched for in a wide variety of processes to probe to the possible underlying sources and CLFV mediation mechanisms.

$$pp \to \ell_\alpha \bar{\ell}_\beta + X$$

$$ep \to \ell + X$$

$$\ell_\alpha \to \ell_\beta \gamma$$

$$J/\psi \to \ell_\alpha \bar{\ell}_\beta$$

$$B^0, K^0 \to \ell_\alpha \bar{\ell}_\beta$$

$$\mu + N \to e + N$$

Charged Lepton Flavor Violation Limits

- Present and future limits:

Process	Experiment	Limit $(90\%\ C.L.)$	Year
$\mu \to e\gamma$	MEGA	$Br < 1.2 \times 10^{-11}$	2002
$\mu + Au \to e + Au$	SINDRUM II	$\Gamma_{conv}/\Gamma_{capt} < 7.0 \times 10^{-13}$	2006
$\mu \to 3e$	SINDRUM	$Br < 1.0 \times 10^{-12}$	1988
$\tau \to e\gamma$	BaBar	$Br < 3.3 \times 10^{-8}$	2010
$\tau \to \mu\gamma$	BaBar	$Br < 6.8 \times 10^{-8}$	2005
$\tau \to 3e$	BELLE	$Br < 3.6 \times 10^{-8}$	2008
$\mu + N \to e + N$	Mu2e	$\Gamma_{conv}/\Gamma_{capt} < 6.0 \times 10^{-17}$	2017?
$\mu \to e\gamma$	MEG	$Br \lesssim 10^{-13}$	2011?
$\tau \to e\gamma$	Super-B	$Br \lesssim 10^{-10}$	> 2020?

- Note that CLFV(1,2) is severely constrained. Limits on CLFV(1,3) are weaker by several orders of magnitude.
- Limits on CLFV(1,2) are expected to improve even further in future experiments.

Snowmass 2021 White Paper

[2203.14919 Banergee et. al.]

- Snowmass report focused on CLFV involving the tau lepton:

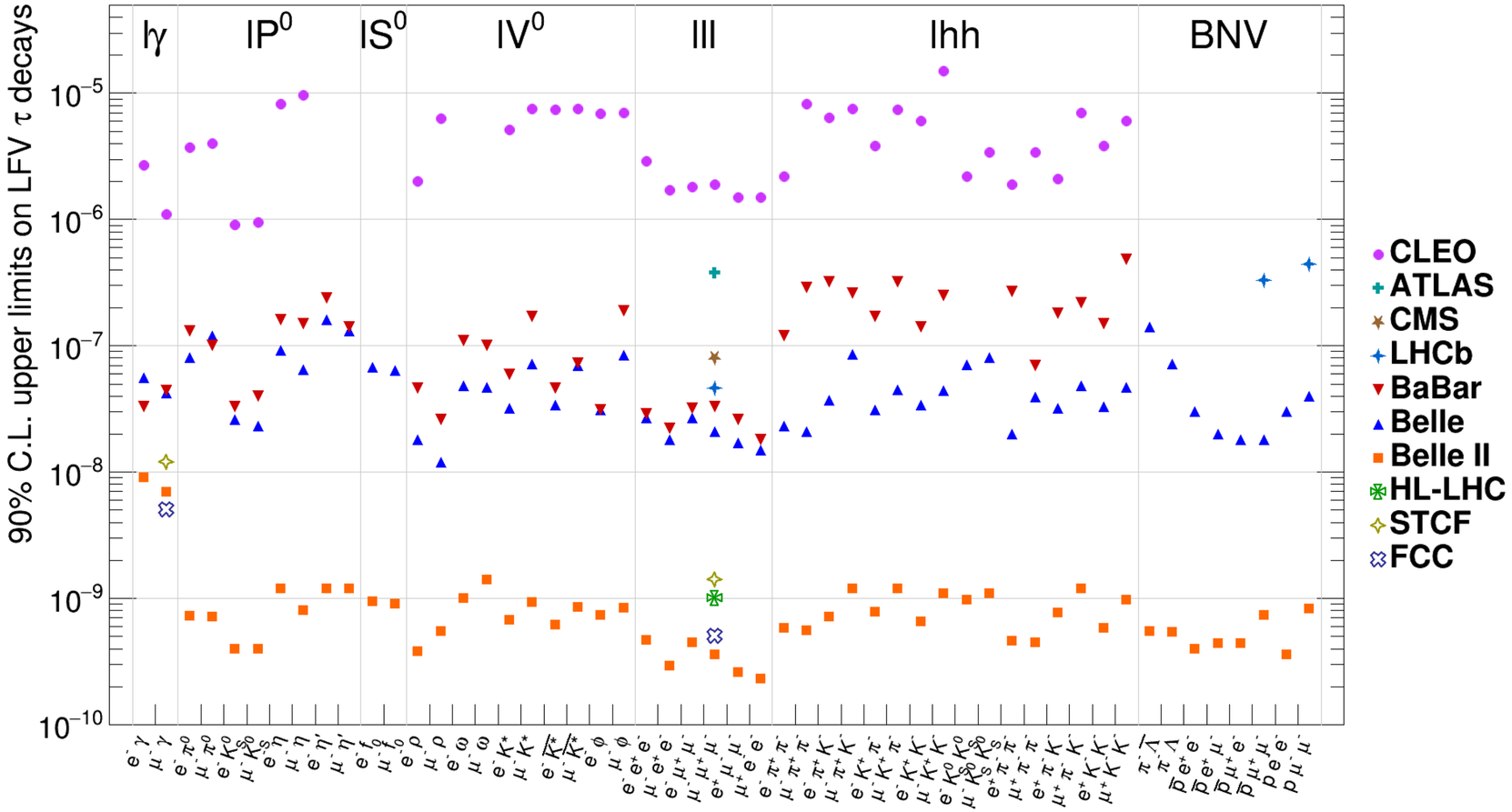

Figure 3: Summary of upper limits on LFV processes in τ decays.

Snowmass 2021 White Paper

[2203.14919 Banergee et. al.]

- SMEFT analysis to constrain CLFV operators: [2102.06176, Cirigliano, Fuyuto, Lee, Mereghetti, Yan]

$$[C_{Ld}]_{ij}\frac{4G_{\rm F}}{\sqrt{2}}\bar{\ell}_\tau\gamma^\mu\ell_e\bar{d}_i\gamma_\mu d_j$$

$$\Gamma^e_\gamma\frac{e}{2v}\bar{\tau}_L\sigma^{\mu\nu}e_R F_{\mu\nu}$$

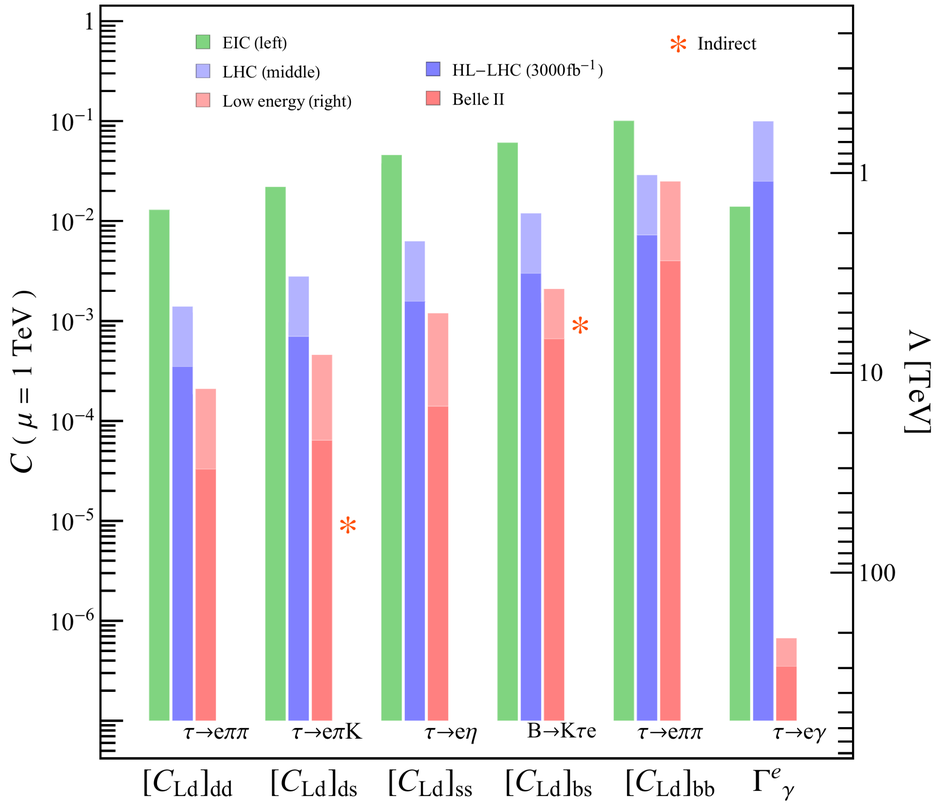

Figure 4: Upper limits on $[C_{Ld}]_{\tau e}$ and Γ^e_γ operators from the EIC (green, left), LHC (blue, middle) and low-energy τ and B meson decays (pink, right). The rightmost vertical axis depicts the lower limit on the scale of new physics Λ. The light pink and blue bars denote existing limits from τ and B decays from the B-factories and other low energy experiments, and from LFV Drell Yan at the LHC, respectively. The darker blue and pink bars overlaid on the lighter ones are the expected sensitivity at the HL-LHC and Belle II. Indirect bounds originating from charged-current decays and meson decays to neutrinos are indicated by an asterisk in orange.

CLFV(1,3) in at EIC

[M.Gonderinger, M.Ramsey-Musolf]

[ECCE Collaboration]

[Cirigliano, Fuyuto,Lee,Mereghetti,Yan]

- The EIC can search for CLFV(1,3) in the DIS process:

$$ep \to \tau X$$

- Final EIC sensitivity depends on the ability to identify this signal over enormous standard model backgrounds.

CLFV in Leptoquark Framework

[M.Gonderinger, M.Ramsey-Musolf]

- The EIC can search for CLFV(1,3) in the DIS process:

$$ep \to \tau X$$

- Such a process could be mediated, for example, by leptoquarks:

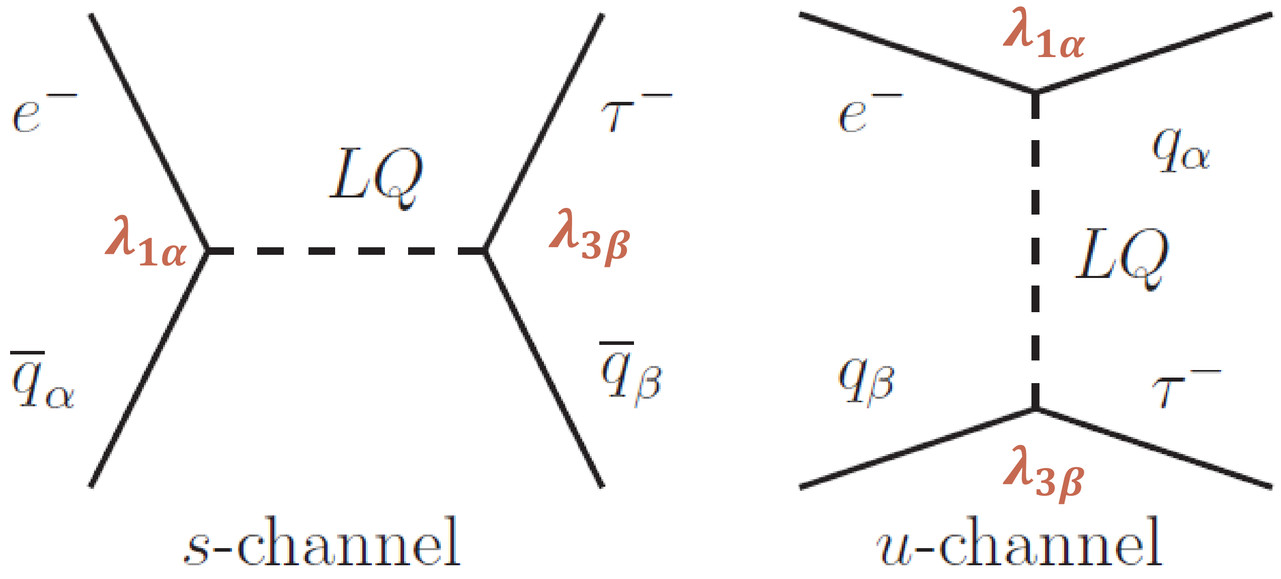

- CLFV can also be studied in the SMEFT framework

[Cirigliano, Fuyuto,Lee,Mereghetti,Yan]

Leptoquarks

- Renormalizable and gauge invariant couplings of LQs to quarks and leptons:

$$\begin{aligned}\mathcal{L}_{F=0} &= h^L_{1/2}\overline{u}_R\ell_L S^L_{1/2} + h^R_{1/2}\overline{q}_L\epsilon e_R S^R_{1/2} + \tilde{h}^L_{1/2}\overline{d}_R\ell_L\tilde{S}^L_{1/2} + h^L_0\overline{q}_L\gamma_\mu\ell_L V_0^{L\mu} \\ &\quad + h^R_0\overline{d}_R\gamma_\mu e_R V_0^{R\mu} + \tilde{h}^R_0\overline{u}_R\gamma_\mu e_R\tilde{V}_0^{R\mu} + h^L_1\overline{q}_L\gamma_\mu\vec{\tau}\ell_L\vec{V}_1^{L\mu} + \text{h.c.}\end{aligned}$$

$$\begin{aligned}\mathcal{L}_{|F|=2} &= g^L_0\overline{q}^c_L\epsilon\ell_L S^L_0 + g^R_0\overline{u}^c_R e_R S^R_0 + \tilde{g}^R_0\overline{d}^c_R e_R\tilde{S}^R_0 + g^L_1\overline{q}^c_L\epsilon\vec{\tau}\ell_L\vec{S}^L_1 + g^L_{1/2}\overline{d}^c_R\gamma_\mu\ell_L V^{L\mu}_{1/2} \\ &\quad + g^R_{1/2}\overline{q}^c_L\gamma_\mu e_R V^{R\mu}_{1/2} + \tilde{g}^L_{1/2}\overline{u}^c_R\gamma_\mu\ell_L\tilde{V}^{L\mu}_{1/2} + \text{h.c.}\end{aligned}$$

- Classification of the 14 types of LQs: [Buchmuller, Ruckl, Wyler (BRW)]

Type	J	F	Q	ep dominant process	Coupling	Branching ratio β_ℓ
S_0^L	0	2	$-1/3$	$e_L^- u_L \to \ell^- u$	λ_L	1/2
				$e_L^- u_L \to \nu_\ell d$	$-\lambda_L$	1/2
S_0^R	0	2	$-1/3$	$e_R^- u_R \to \ell^- u$	λ_R	1
$\tilde{S}_0^R$	0	2	$-4/3$	$e_R^- d_R \to \ell^- d$	λ_R	1
S_1^L	0	2	$-1/3$	$e_L^- u_L \to \ell^- u$	$-\lambda_L$	1/2
				$e_L^- u_L \to \nu_\ell d$	$-\lambda_L$	1/2
			$-4/3$	$e_L^- d_L \to \ell^- d$	$-\sqrt{2}\lambda_L$	1
$V_{1/2}^L$	1	2	$-4/3$	$e_L^- d_R \to \ell^- d$	λ_L	1
$V_{1/2}^R$	1	2	$-1/3$	$e_R^- u_L \to \ell^- u$	λ_R	1
			$-4/3$	$e_R^- d_L \to \ell^- d$	λ_R	1
$\tilde{V}_{1/2}^L$	1	2	$-1/3$	$e_L^- u_R \to \ell^- u$	λ_L	1

Type	J	F	Q	ep dominant process	Coupling	Branching ratio β_ℓ
V_0^L	1	0	$+2/3$	$e_R^+ d_L \to \ell^+ d$	λ_L	1/2
				$e_R^+ d_L \to \bar{\nu}_\ell u$	λ_L	1/2
V_0^R	1	0	$+2/3$	$e_L^+ d_R \to \ell^+ d$	λ_R	1
$\tilde{V}_0^R$	1	0	$+5/3$	$e_L^+ u_R \to \ell^+ u$	λ_R	1
V_1^L	1	0	$+2/3$	$e_R^+ d_L \to \ell^+ d$	$-\lambda_L$	1/2
				$e_R^+ d_L \to \bar{\nu}_\ell u$	λ_L	1/2
			$+5/3$	$e_R^+ u_L \to \ell^+ u$	$\sqrt{2}\lambda_L$	1
$S_{1/2}^L$	0	0	$+5/3$	$e_R^+ u_R \to \ell^+ u$	λ_L	1
$S_{1/2}^R$	0	0	$+2/3$	$e_L^+ d_L \to \ell^+ d$	$-\lambda_R$	1
			$+5/3$	$e_L^+ u_L \to \ell^+ u$	λ_R	1
$\tilde{S}_{1/2}^L$	0	0	$+2/3$	$e_R^+ d_R \to \ell^+ d$	λ_L	1

Leptoquarks

[Buchmuller, Ruckl, Wyler (BRW)]

Type	J	F	Q	ep dominant process	Coupling	Branching ratio β_ℓ
S_0^L	0	2	$-1/3$	$e_L^- u_L \to \ell^- u$	λ_L	1/2
				$\nu_\ell d$	$-\lambda_L$	1/2
S_0^R	0	2	$-1/3$	$e_R^- u_R \to \ell^- u$	λ_R	1
$\tilde{S}_0^R$	0	2	$-4/3$	$e_R^- d_R \to \ell^- d$	λ_R	1
S_1^L	0	2	$-1/3$	$e_L^- u_L \to \ell^- u$	$-\lambda_L$	1/2
				$\nu_\ell d$	$-\lambda_L$	1/2
			$-4/3$	$e_L^- d_L \to \ell^- d$	$-\sqrt{2}\lambda_L$	1
$V_{1/2}^L$	1	2	$-4/3$	$e_L^- d_R \to \ell^- d$	λ_L	1
$V_{1/2}^R$	1	2	$-1/3$	$e_R^- u_L \to \ell^- u$	λ_R	1
			$-4/3$	$e_R^- d_L \to \ell^- d$	λ_R	1
$\tilde{V}_{1/2}^L$	1	2	$-1/3$	$e_L^- u_R \to \ell^- u$	λ_L	1

Type	J	F	Q	ep dominant process	Coupling	Branching ratio β_ℓ
V_0^L	1	0	$+2/3$	$e_R^+ d_L \to \ell^+ d$	λ_L	1/2
				$\bar{\nu}_\ell u$	λ_L	1/2
V_0^R	1	0	$+2/3$	$e_L^+ d_R \to \ell^+ d$	λ_R	1
$\tilde{V}_0^R$	1	0	$+5/3$	$e_L^+ u_R \to \ell^+ u$	λ_R	1
V_1^L	1	0	$+2/3$	$e_R^+ d_L \to \ell^+ d$	$-\lambda_L$	1/2
				$\bar{\nu}_\ell u$	λ_L	1/2
			$+5/3$	$e_R^+ u_L \to \ell^+ u$	$\sqrt{2}\lambda_L$	1
$S_{1/2}^L$	0	0	$+5/3$	$e_R^+ u_R \to \ell^+ u$	λ_L	1
$S_{1/2}^R$	0	0	$+2/3$	$e_L^+ d_L \to \ell^+ d$	$-\lambda_R$	1
			$+5/3$	$e_L^+ u_L \to \ell^+ u$	λ_R	1
$\tilde{S}_{1/2}^L$	0	0	$+2/3$	$e_R^+ d_R \to \ell^+ d$	λ_L	1

- In order to maximally exploit the phenomenology of LQs and be able to distinguish between different types of LQ states, we need:

-electron and positron beams [separate |F|=0 vs |F|=2]
-proton and deuteron targets [separate "eu" vs "ed" LQs]
-polarized beams [separate L vs R]
-wide kinematic range [separate scalar vs vector LQs]

CLFV mediated by Leptoquarks

- Cross-section for $ep \to \tau X$ takes the form:

$$\sigma_{F=0} = \sum_{\alpha,\beta} \frac{s}{32\pi} \left[\frac{\lambda_{1\alpha}\lambda_{3\beta}}{M_{LQ}^2} \right]^2 \left\{ \int dxdy\; x\bar{q}_\alpha\left(x, xs\right) f\left(y\right) + \int dxdy\; xq_\beta\left(x, -u\right) g\left(y\right) \right\}$$

$$f\left(y\right) = \begin{cases} 1/2 & \text{(scalar)} \\ 2\left(1-y\right)^2 & \text{(vector)} \end{cases}, \quad g\left(y\right) = \begin{cases} \left(1-y\right)^2/2 & \text{(scalar)} \\ 2 & \text{(vector)} \end{cases}$$

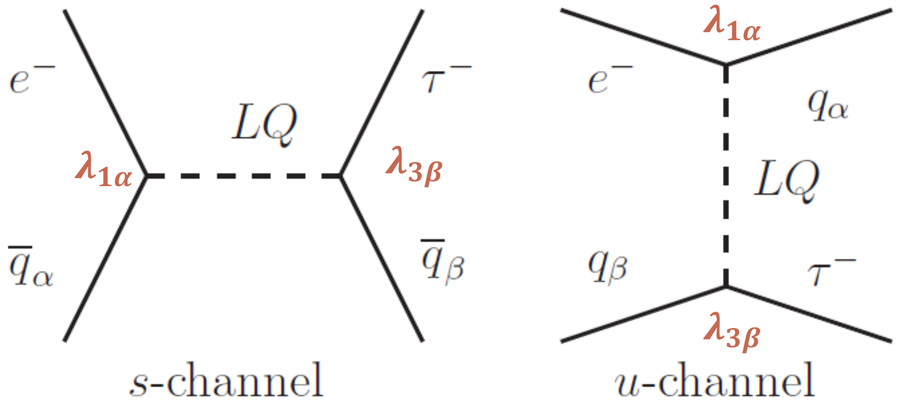

$F = 0$

- HERA set limits on the ratios $\frac{\lambda_{1\alpha}\lambda_{3\beta}}{M_{LQ}^2}$
  - all LQs
  - all combinations of quark generations (no top quarks)
  - degenerate masses assumed for LQ multiplets

[S. Chekanov et.al (ZEUS), A.Atkas et.al (H1)]

Tree-Level Cross Sections For Leptoquark Mediated CLFV

$$\sigma_{F=0} = \sum_{\alpha,\beta} \frac{s}{32\pi} \left[\frac{\lambda_{1\alpha}\lambda_{3\beta}}{M_{LQ}^2} \right]^2 \left\{ \int dxdy\; x\bar{q}_\alpha\left(x, xs\right) f\left(y\right) + \int dxdy\; xq_\beta\left(x, -u\right) g\left(y\right) \right\}$$

- Limits can be set on the contact interaction factor:

$$\chi\alpha\beta \equiv \frac{\lambda_{1\alpha}\lambda_{2\beta}}{M_{LQ}^2}$$

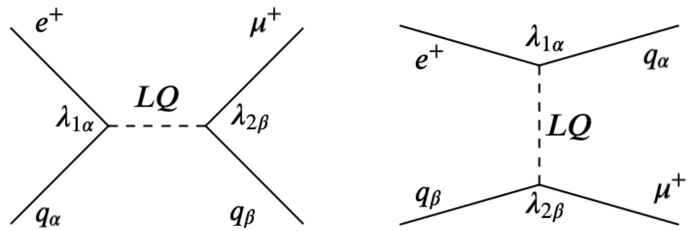

- It becomes useful to define the ratio of the contact interaction factor to its HERA limit. The cross section can now be thought of as a function of z:

$$z \equiv \frac{\chi\alpha\beta}{\chi_{\alpha\beta}^{\mathrm{HERA}}}$$

- Any obtained limit of $z < 1$, would signal an improvement over the HERA limit.

[S. Chekanov et.al (ZEUS), A.Atkas et.al (H1)]

CLFV(1,3) in at EIC

[ECCE Collaboration]

- The EIC Comprehensive Chromodynamics Experiment (ECCE) detector concept was used to provide realistic detector simulations to project the EIC sensitivity to CLFV(1,3):

$$ep \to \tau X$$

- tau decay modes are classified into 1-prong and 3-prong modes:

1-prong (one charged particle in decay)

$$\tau^- \to e^- \bar{\nu}_e \nu_\tau$$

$$\tau^- \to \mu^- \bar{\nu}_\mu \nu_\tau$$

$$\tau^- \to \nu_\tau \pi^-$$

(~85%)

3-prong (three charged particles in decay)

$$\tau^- \to \nu_\tau \pi^- \pi^+ \pi^-$$

(~15%)

CLFV(1,3) in at EIC

[ECCE Collaboration]

- The EIC Comprehensive Chromodynamics Experiment (ECCE) detector concept was used to provide realistic detector simulations to project the EIC sensitivity to CLFV(1,3):

$$ep \to \tau X$$

- tau decay modes are classified into 1-prong and 3-prong modes:

1-prong (one charged particle in decay)

$$\tau^- \to e^- \bar{\nu}_e \nu_\tau$$

$$\tau^- \to \mu^- \bar{\nu}_\mu \nu_\tau$$

$$\tau^- \to \nu_\tau \pi^-$$

(~85%)

3-prong (three charged particles in decay)

Focus of this study

$$\tau^- \to \nu_\tau \pi^- \pi^+ \pi^-$$

(~15%)

Features of the 3-Prong Decay Mode

[ECCE Collaboration]

Focus of this study

$$\tau^- \rightarrow \nu_\tau \pi^- \pi^+ \pi^-$$

(~15%)

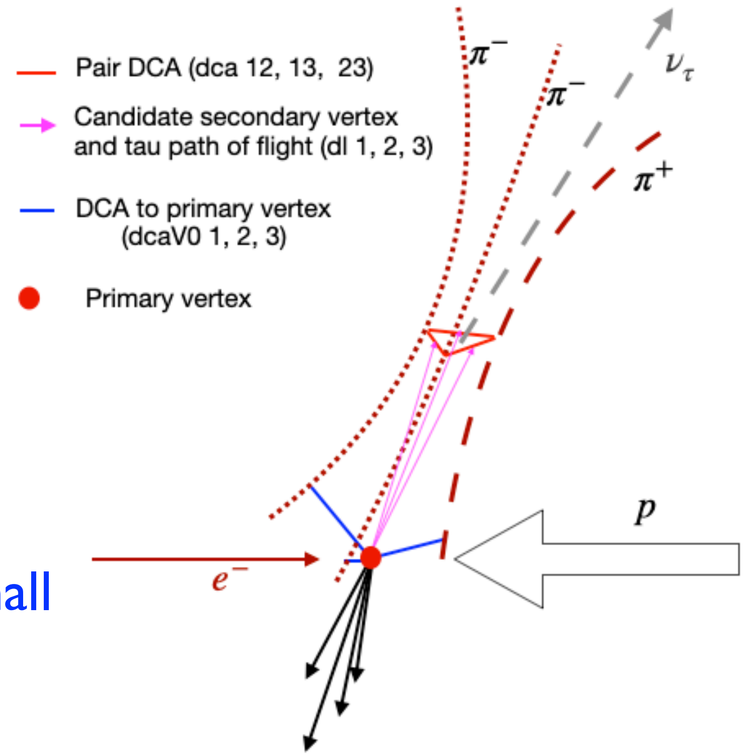

- No scattered electron detected
- High-pT tau-jet with three charged particles within a relatively small cone
- Displaced vertex from which three charged particles emerge
- High-pT hadronic jet recoiling against tau jet
- pT-imbalance due to undetected neutrino

SM backgrounds:

- NC DIS, CC DIS, photoproduction

Set up used for Analysis

[ECCE Collaboration]

Focus of this study

$$\tau^- \longrightarrow \nu_\tau \pi^- \pi^+ \pi^-$$

(~15%)

$18 \times 275\ \mathrm{GeV}$, ep collision

$M_{\mathrm{LQ}} = 1.9\ \mathrm{TeV}$

$Q^2 > 10\ \mathrm{GeV}^2$

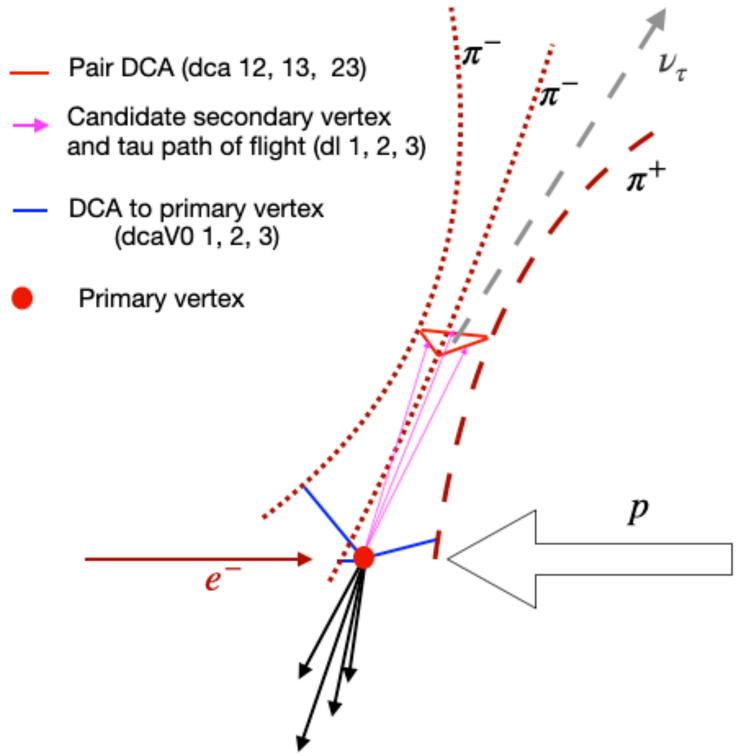

- LQGENEP used to generate signal events
- Djangoh and Pythia used to generate NC and CC DIS and photo production events, respectively
- Generated events passed through ECCE GEANT4 detector simulation

Set up used for Analysis

[ECCE Collaboration]

Focus of this study

$$\tau^- \rightarrow \nu_\tau \pi^- \pi^+ \pi^-$$

(~15%)

$18 \times 275\ \mathrm{GeV}$, ep collision

$M_{\mathrm{LQ}} = 1.9\ \mathrm{TeV}$

$Q^2 > 10\ \mathrm{GeV}^2$

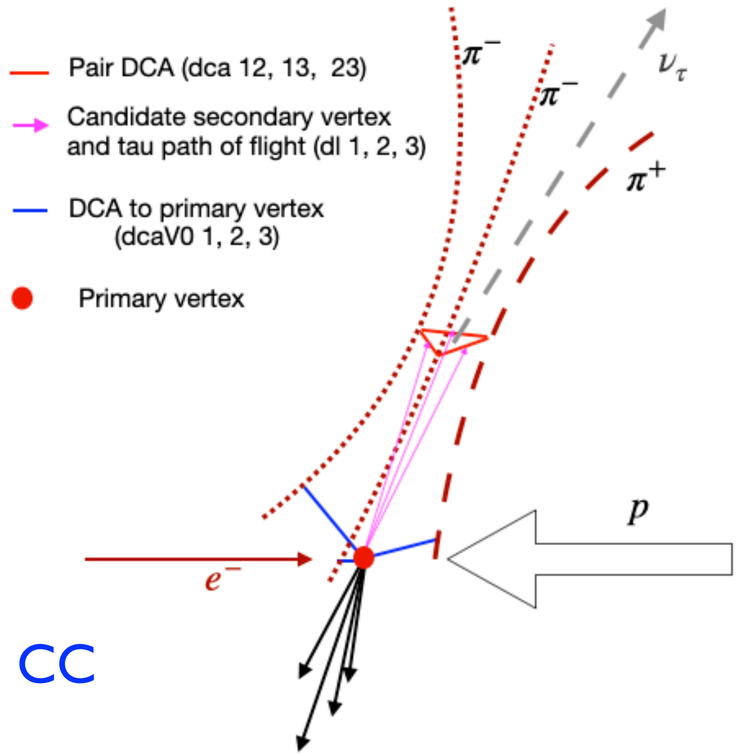

- LQGENEP [Bellagamba 2001] used to generate signal events
- Djangoh [Spiesberger 2001] and Pythia used to generate NC and CC DIS and photo production events, respectively
- Generated events passed through ECCE GEANT4 detector simulation
- Charged pion tracking info is from simulated tracking and detector responses
- PID for charged pions is from generator level (i.e. perfect PID is assumed)

[EIC/ECCE Collaboration]

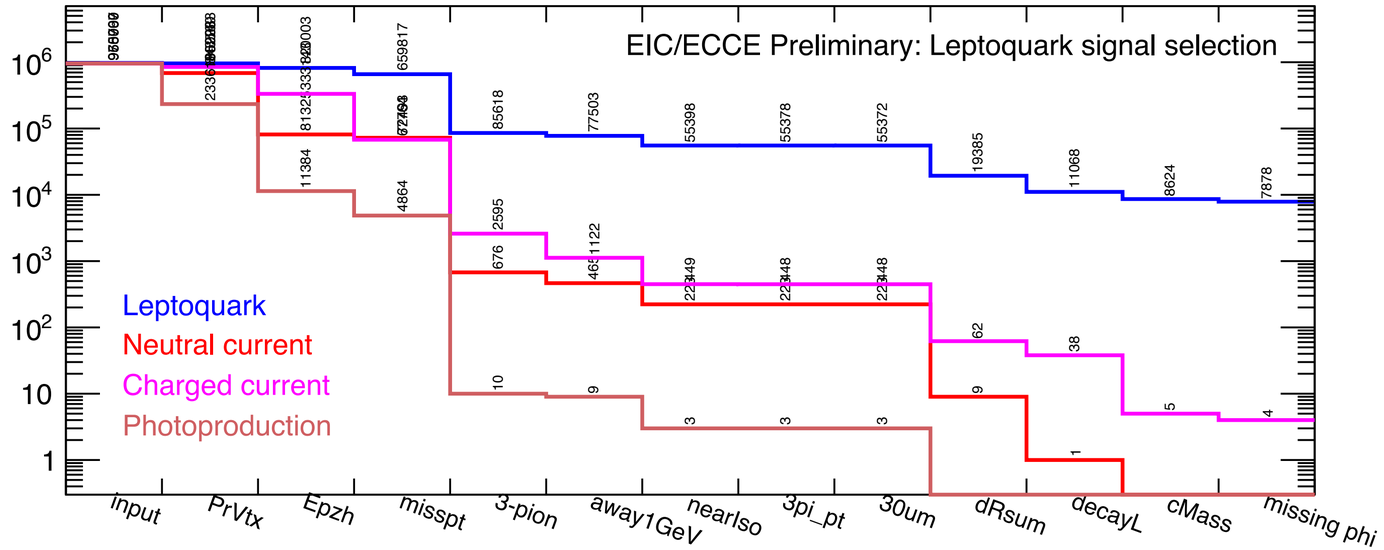

Figure 4: MC statistics of leptoquark (blue), DIS CC (red), DIS NC (magenta), and photoproduction (orange) events, as ten selection criteria are progressively applied on 1 M input events for each channel. Please see text for details.

- Simulated $1M$ events for each of the signal and background processes
- For 100fb^{-1} this corresponds to particular cross section sizes for the signal and background events.
- The number of selected events in each background channel is then scaled to the true cross section value.
- The number of selected signal events is scaled to the required number that satisfies:

$$S / \sqrt{(B)} \geq 5$$

- This scaled number of signal events corresponds to a signal cross section at 100fb^{-1} which corresponds to the needed EIC signal cross section sensitivity.

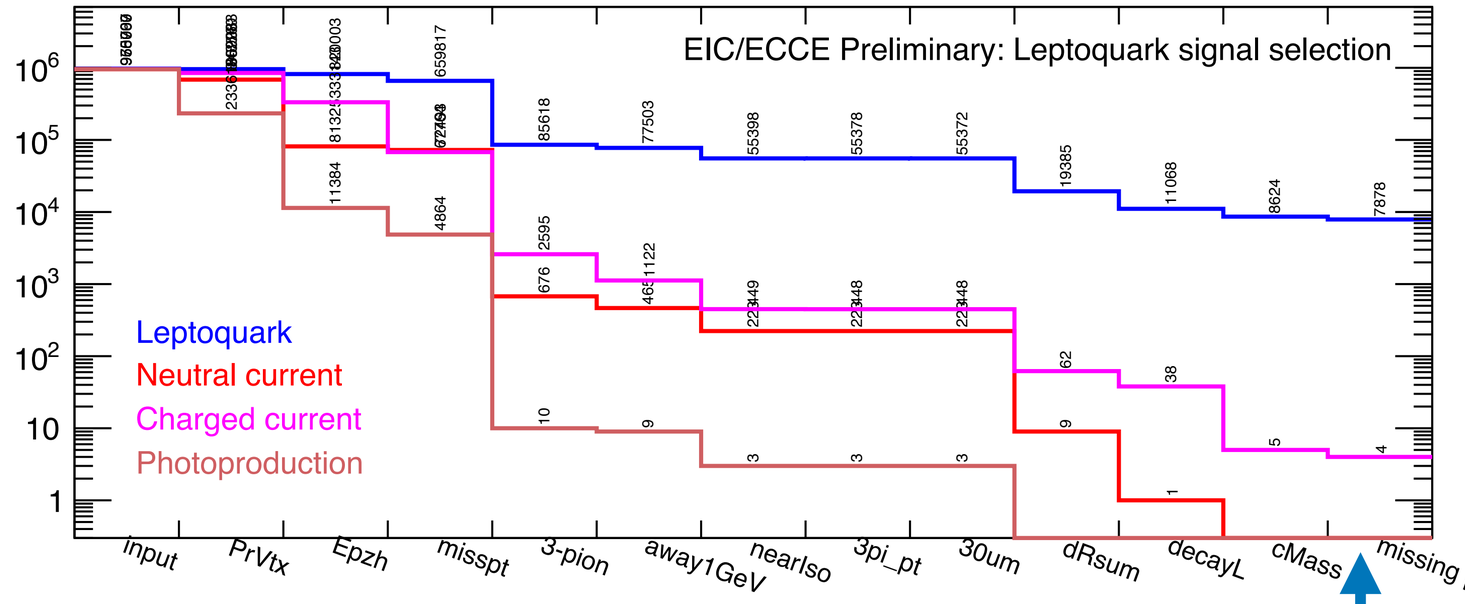

Figure 4: MC statistics of leptoquark (blue), DIS CC (red), DIS NC (magenta), and photoproduction (orange) events, as ten selection criteria are progressively applied on 1 M input events for each channel. Please see text for details.

Zero background events survive for NC DIS and Photoproduction

Need 1B simulation events to match the true cross sections for NC DIS + phototoproduction to see how many background events survive.

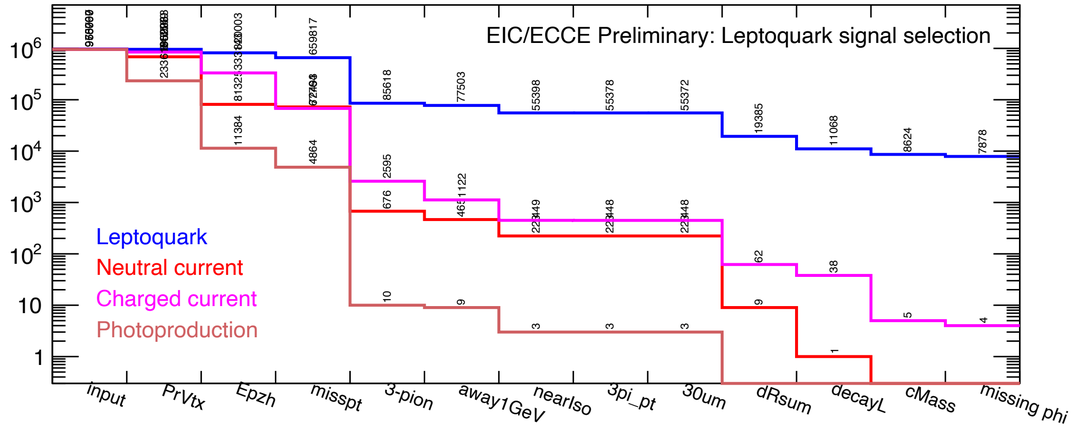

Figure 4: MC statistics of leptoquark (blue), DIS CC (red), DIS NC (magenta), and photoproduction (orange) events, as ten selection criteria are progressively applied on 1 M input events for each channel. Please see text for details.

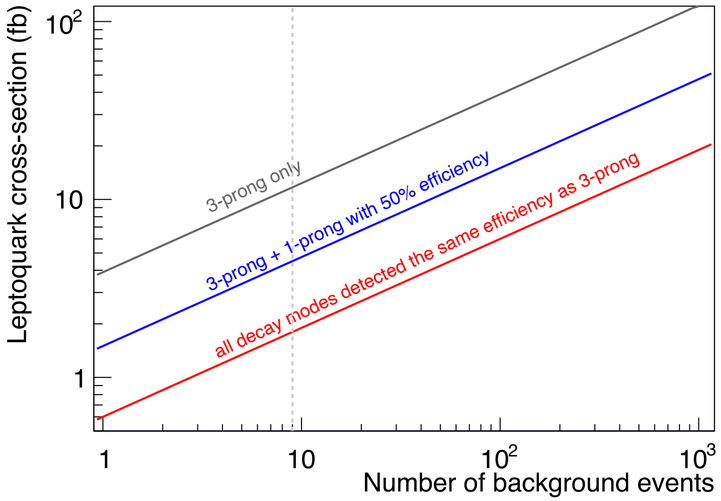

Figure 6: Cross section sensitivity for leptoquark search vs number of residual background events for 100 fb^{-1} integrated luminosity. The grey line corresponds to the scenario that only “3-prong" decay modes are detected. The blue line corresponds to the scenario where electron and pion “1-prong" decay modes could be detected with 50% efficiency of the “3-prong" case. And the red line shows the scenario if all decay modes were detected at the same efficiency as the “3-prong” case.

EIC sensitivity to signal cross section as a function of the number of background events that survive.

$$S / \sqrt{(B)} \geq 5$$

[EIC/ECCE Collaboration]

$$\sigma_{F=0} = \sum_{\alpha,\beta} \frac{s}{32\pi} \left[\frac{\lambda_{1\alpha}\lambda_{3\beta}}{M_{LQ}^2} \right]^2 \left\{ \int dxdy\ x\bar{q}_\alpha(x, xs)\, f(y) + \int dxdy\ xq_\beta(x, -u)\, g(y) \right\}$$

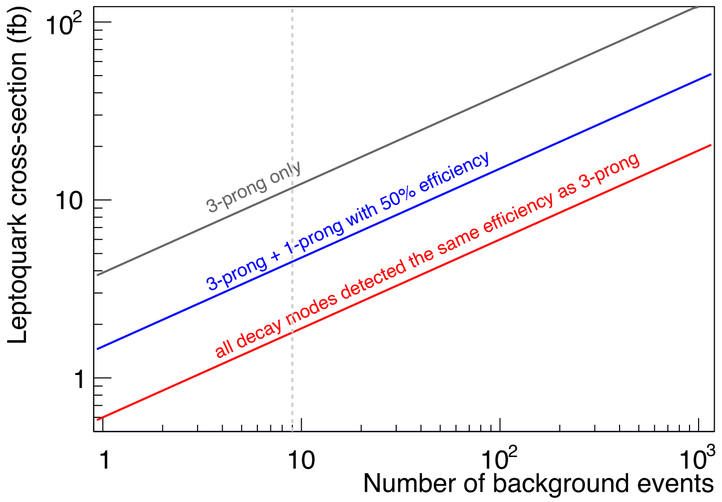

Figure 6: Cross section sensitivity for leptoquark search vs number of residual background events for 100 fb^{-1} integrated luminosity. The grey line corresponds to the scenario that only "3-prong" decay modes are detected. The blue line corresponds to the scenario where electron and pion "1-prong" decay modes could be detected with 50% efficiency of the "3-prong" case. And the red line shows the scenario if all decay modes were detected at the same efficiency as the "3-prong" case.

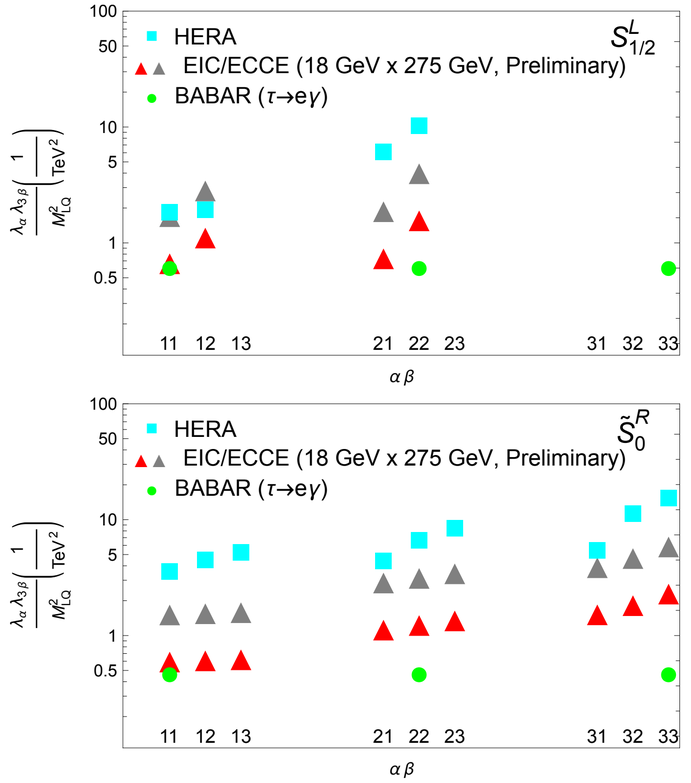

Figure 7: Limits on the scalar leptoquarks with $F = 0$ $S^L_{1/2}$ (top) and $|F| = 2$ $\tilde{S}^R_0$ (bottom) from 100 fb^{-1} of ep 18×275 GeV data, based on a sensitivity to leptoquark-mediated $ep \to \tau X$ cross section of size 1.7 fb (red triangles) or 11.4 fb (grey triangles) with ECCE. Note that due to small value of $\sqrt{s}$, EIC cannot constraint the third generation couplings of $S^L_{1/2}$ to top quarks. Limits from HERA [11, 5, 12, 6] are shown as cyan solid squares, and limits from $\tau \to e\gamma$ decays [3] are shown as green solid circles.

[EIC/ECCE Collaboration]

$$\sigma_{F=0} = \sum_{\alpha,\beta} \frac{s}{32\pi} \left[\frac{\lambda_{1\alpha}\lambda_{3\beta}}{M_{LQ}^2} \right]^2 \left\{ \int dxdy\ x\bar{q}_\alpha(x, xs)\, f(y) + \int dxdy\ xq_\beta(x, -u)\, g(y) \right\}$$

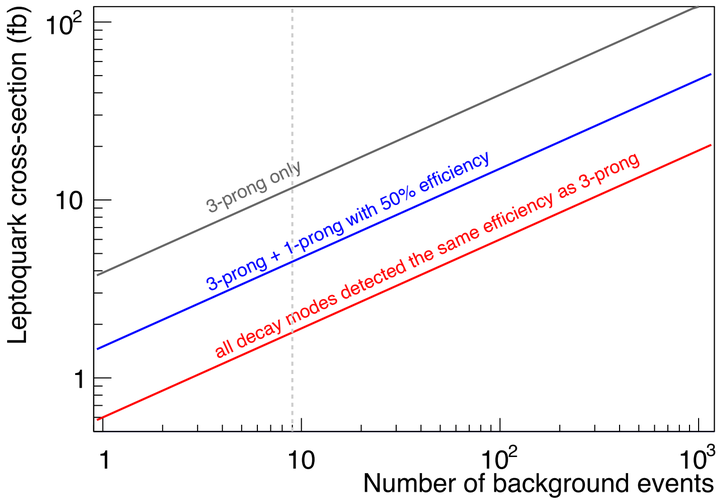

Figure 6: Cross section sensitivity for leptoquark search vs number of residual background events for 100 fb^{-1} integrated luminosity. The grey line corresponds to the scenario that only "3-prong" decay modes are detected. The blue line corresponds to the scenario where electron and pion "1-prong" decay modes could be detected with 50% efficiency of the "3-prong" case. And the red line shows the scenario if all decay modes were detected at the same efficiency as the "3-prong" case.

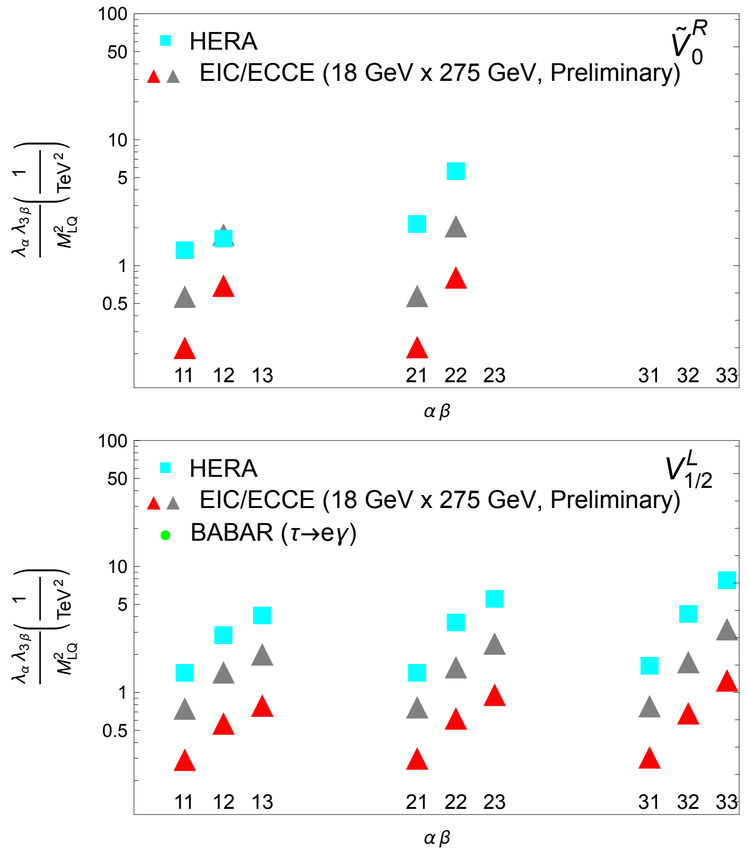

Figure 8: Limits on the vector leptoquarks with $F = 0$ $\tilde{V}_0^R$ (top) and $|F| = 2$ $V_{1/2}^L$ (bottom) from 100 fb^{-1} of ep 18 × 275 GeV data, based on a sensitivity to leptoquark-mediated $ep \to \tau X$ cross section of size 1.7 fb (red triangles) or 11.4 fb (grey triangles) from ECCE. Note that due to small value of $\sqrt{s}$, EIC cannot constraint the third generation couplings of $\tilde{V}_0^R$ to top quarks. Limits from HERA [11, 5, 12, 6] are shown as cyan solid squares. Limits from $\tau \to e\gamma$ decays [3] exist but require some work to convert to the 4-fermion contact term. This will be done in the future.

CLFV(1,2) in DIS

[Furletova, SM]

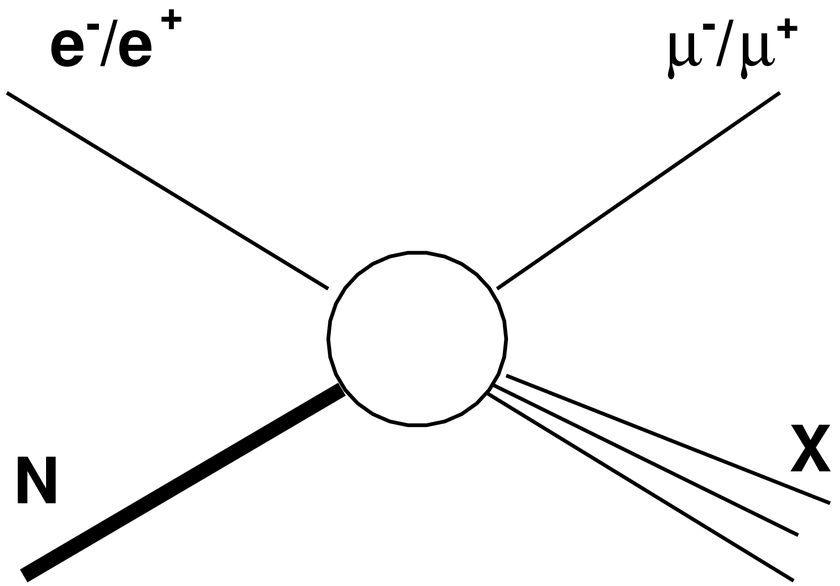

$$e^{\pm} + N \rightarrow \mu^{\pm} + X$$

- One can also search for CLFV(1,2) in the DIS process, which can probe different CLFV mechanisms and is complementary to the other low energy experiments.

- There are already CLFV(1,2) limits from the $H1$ and ZEUS collaborations at HERA. For example, the $H1$ collaboration made searches for the settings: [S. Chekanov et.al (ZEUS), A.Atkas et.al (H1)]

$$\sqrt{s} = 319\ \text{GeV}$$

$$H1, e^{-}p : \mathscr{L} = 166\ \text{pb}^{-1}$$

$$H1, e^{+}p : \mathscr{L} = 245\ \text{pb}^{-1}$$

CLFV(1,2) in DIS

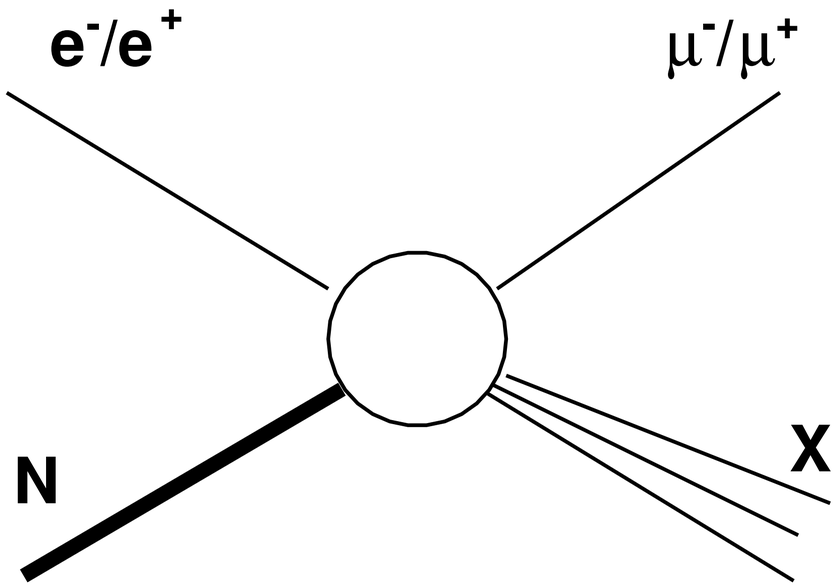

$$e^{\pm} + N \rightarrow \mu^{\pm} + X$$

- One can also set limits on CLFV(1,2) at JLAB:

$$\sqrt{s} = 4.5 \text{ GeV} \qquad \text{JLAB} : \mathscr{L} = 10^{36-39}\,\text{cm}^{-2}\,s^{-1}$$

- Even though the center of mass energy is very small compared to HERA, corresponding to a much lower mass reach, the much larger luminosity could allow for improvement over HERA by up to two orders of magnitude.

- Can complement searches at NA64 for $e - \tau$ and $\mu - \tau$ transitions.

Preliminary Estimate of CLFV Limits with a Positron Beam at JLAB

[Furletova, SM]

Type	J	F	Q	ep dominant process	Coupling	Branching ratio β_ℓ
S_0^L	0	2	$-1/3$	$e_L^- u_L \to \ell^- u$	λ_L	1/2
				$e_L^- u_L \to \nu_\ell d$	$-\lambda_L$	1/2
S_0^R	0	2	$-1/3$	$e_R^- u_R \to \ell^- u$	λ_R	1
$\tilde{S}_0^R$	0	2	$-4/3$	$e_R^- d_R \to \ell^- d$	λ_R	1
S_1^L	0	2	$-1/3$	$e_L^- u_L \to \ell^- u$	$-\lambda_L$	1/2
				$e_L^- u_L \to \nu_\ell d$	$-\lambda_L$	1/2
			$-4/3$	$e_L^- d_L \to \ell^- d$	$-\sqrt{2}\lambda_L$	1
$V_{1/2}^L$	1	2	$-4/3$	$e_L^- d_R \to \ell^- d$	λ_L	1
$V_{1/2}^R$	1	2	$-1/3$	$e_R^- u_L \to \ell^- u$	λ_R	1
			$-4/3$	$e_R^- d_L \to \ell^- d$	λ_R	1
$\tilde{V}_{1/2}^L$	1	2	$-1/3$	$e_L^- u_R \to \ell^- u$	λ_L	1

Type	J	F	Q	ep dominant process	Coupling	Branching ratio β_ℓ
V_0^L	1	0	$+2/3$	$e_R^+ d_L \to \ell^+ d$	λ_L	1/2
				$e_R^+ d_L \to \bar{\nu}_\ell u$	λ_L	1/2
V_0^R	1	0	$+2/3$	$e_L^+ d_R \to \ell^+ d$	λ_R	1
$\tilde{V}_0^R$	1	0	$+5/3$	$e_L^+ u_R \to \ell^+ u$	λ_R	1
V_1^L	1	0	$+2/3$	$e_R^+ d_L \to \ell^+ d$	$-\lambda_L$	1/2
				$e_R^+ d_L \to \bar{\nu}_\ell u$	λ_L	1/2
			$+5/3$	$e_R^+ u_L \to \ell^+ u$	$\sqrt{2}\lambda_L$	1
$S_{1/2}^L$	0	0	$+5/3$	$e_R^+ u_R \to \ell^+ u$	λ_L	1
$S_{1/2}^R$	0	0	$+2/3$	$e_L^+ d_L \to \ell^+ d$	$-\lambda_R$	1
			$+5/3$	$e_L^+ u_L \to \ell^+ u$	λ_R	1
$\tilde{S}_{1/2}^L$	0	0	$+2/3$	$e_R^+ d_R \to \ell^+ d$	λ_L	1

- Limits based on running for 5 years with instantaneous luminosity of $\mathscr{L} \sim 10^{38}\,\mathrm{cm}^{-2}s^{-1}$. For an integrated luminosity a factor of 10 smaller, there is still substantial room for improvement over HERA limits.

- Thus, JLAB could improve on HERA limits by two or three orders of magnitude: $z \sim [0.005 - 0.05]$

- This estimate will be modified after taking into account acceptance and background effects.

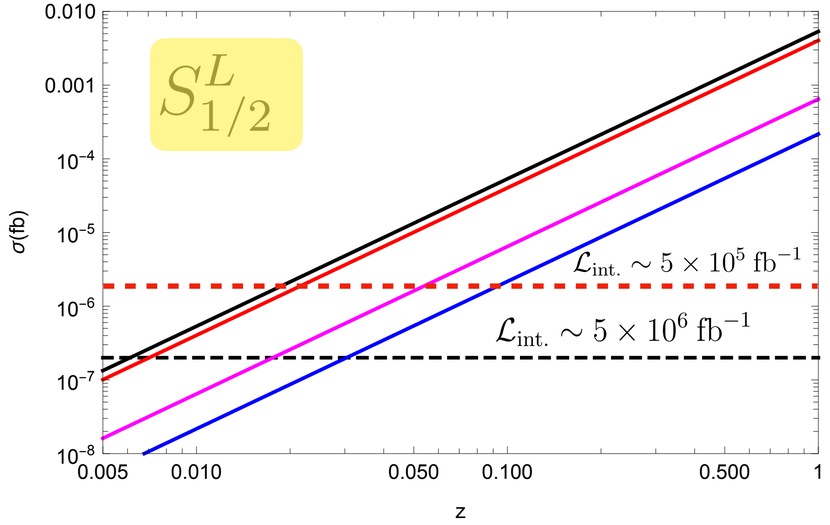

Fig. 5. The cross section for $e^+N \to \mu^+X$ with center of mass energy $\sqrt{s} = 4.5$ GeV, via exchange of the F=0 scalar LQ, $S_{1/2}^L$, as a function of the ratio z defined in Eq. (9). The red, black, magenta, and blue solid lines correspond to the choices $(\alpha, \beta) = \{11, 12, 21, 22\}$ in Eq. (6) with all other terms set to zero. An integrated luminosity of $\mathcal{L} \sim 5 \times 10^6 \mathrm{fb}^{-1}$ will allow sensitivity to cross sections as small as $\sigma \sim 0.2 \times 10^{-6}$ fb (horizontal dashed line).

Conclusions

- The EIC is primarily a QCD machine.

- However, the EIC can also constrain BSM and be complementary to LHC searches and constraints from other low energy experiments. In particular, it can play a significant and complementary role in the search for CLFV. A preliminary analysis was carried out by the ECCE collaboration.

- Such a program physics is facilitated by:

  - high luminosity
  - wide kinematic range
  - range of nuclear targets
  - polarized beams
  - Variety of observables

- High luminosity of fixed target DIS can also provide significant and complementary constraints on CLFV. This was explored in the context of a proposal for a positron beam at JLAB.

Back Up Slides

Experimental Considerations

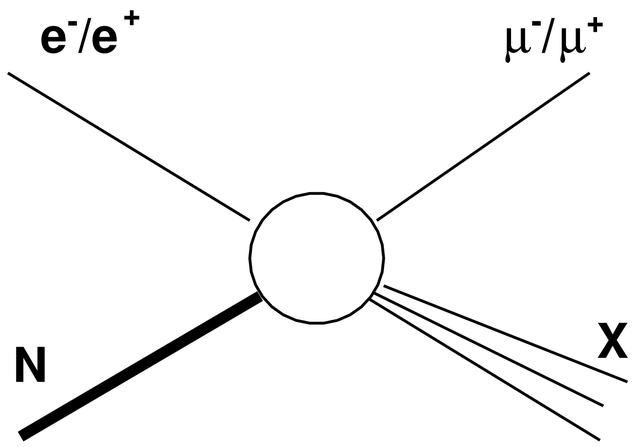

$$\sqrt{s} = 4.5\ \mathrm{GeV}$$

$$\mathscr{L} = 10^{36-39}\ \mathrm{cm}^{-2}\ s^{-1}$$

$$e^{\pm} + N \rightarrow \mu^{\pm} + X$$

- Required experimental capabilities:

-good muon detectors
-good charged particle tracking
-good vertex resolution

SoLID Experiment

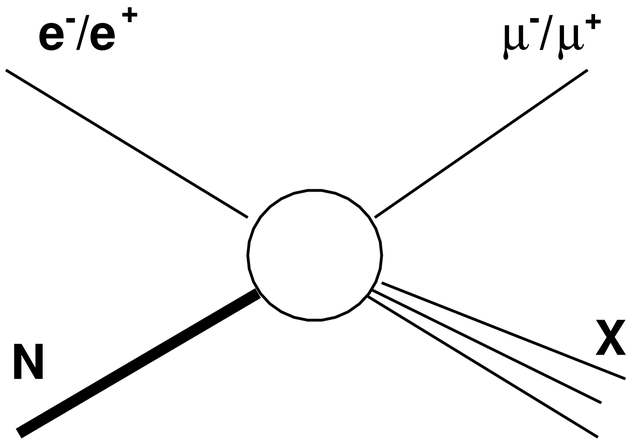

$$e^{\pm} + N \rightarrow \mu^{\pm} + X$$

$$\sqrt{s} = 4.5 \text{ GeV}$$

$$\mathscr{L} = 10^{36-39} \text{ cm}^{-2}\, s^{-1}$$

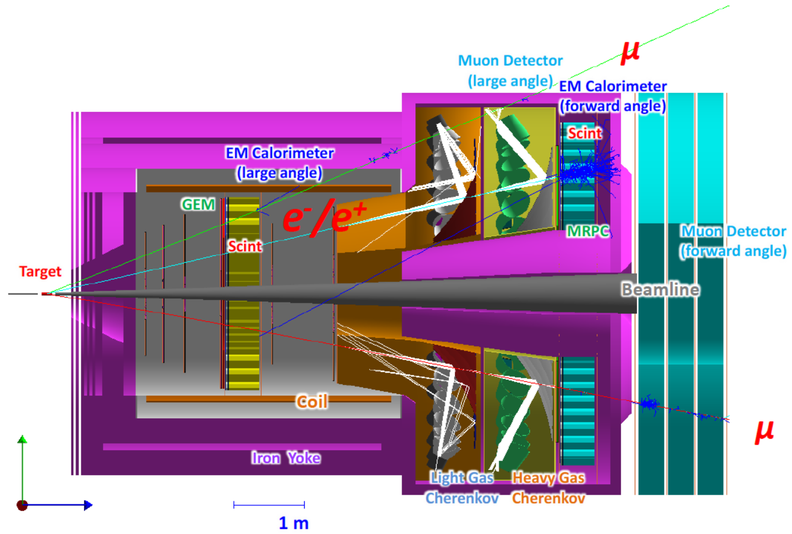

Fig. 3. The SoLID J/Ψ configuration with muon detectors [28]. Other sub-detectors are labeled.

- Polar angle acceptance:

  SIDIS configuration : $\theta = [8^{\circ},24^{\circ}]$

  PVDIS configuration : $\theta = [22^{\circ},35^{\circ}]$

- Azimuthal angle acceptance:

  full-2π acceptance

Most of the cross section is in the forward region due to the kinematic boost of a 11 GeV lepton beam.

SoLID Experiment

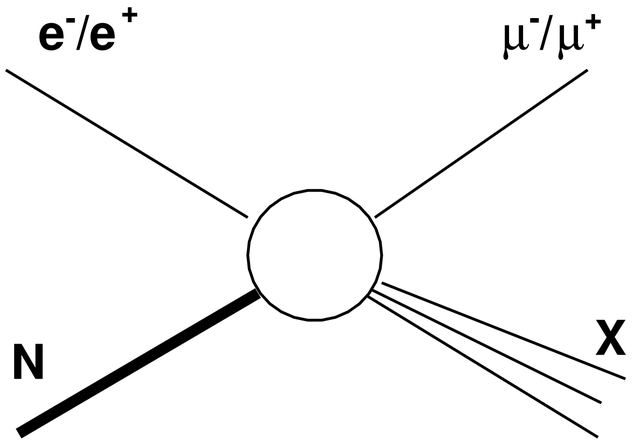

$$e^{\pm} + N \rightarrow \mu^{\pm} + X$$

$$\sqrt{s} = 4.5\ \mathrm{GeV}$$

$$\mathscr{L} = 10^{36-39}\ \mathrm{cm}^{-2}\ s^{-1}$$

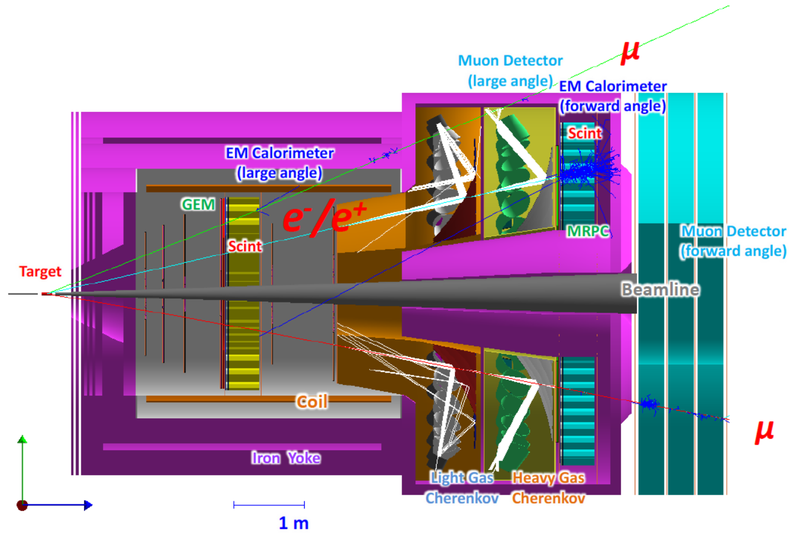

Fig. 3. The SoLID J/Ψ configuration with muon detectors [28]. Other sub-detectors are labeled.

- Muon Chambers:

The J/ψ and DDVCS configurations will be equipped with muon chambers

Muon Backgrounds

- The dominant background to the CLFV signal muon will come from decays of pions to muons:

$$\pi^+ \rightarrow \mu^+ \nu_\mu$$

- This background will be suppressed due to the compact size of of the SoLID detector, so that the typical pion decay length is much bigger than the distance to the detector from their production vertex.

$$P(L) = e^{-L/\lambda_D^\pi}, \qquad \lambda_D^\pi = \frac{p_\pi}{m_\pi c} c\tau,$$

- Pions will be typically produced with momenta in the range:

$$1\ \text{GeV} \lesssim p_\pi \lesssim 7\ \text{GeV}$$

- Thus, the typical pion decay lengths will be in the range:

$$56\ \text{m} \lesssim \lambda_D^\pi \lesssim 390\ \text{m} \quad \gg \quad \sim 5\ \text{m}$$

(Pion decay length)

(Overall detector dimensions, combined with proximity to pion production vertex)

- Correspondingly, the pion survival probability at the detector is:

$p_\pi \sim 1\ \text{GeV} \rightarrow 91\ \%$ survival probabilty

$p_\pi \sim 7\ \text{GeV} \rightarrow 99\ \%$ survival probabilty

Muon Backgrounds

- Charged particle tracking spatial resolution of 100 microns, allowing for precise reconstruction of pion decay vertices to further suppress backgrounds.:

- Other backgrounds can arise from charmed meson decays or J/ψ decays. Once again tracking and vertex resolution capabilities can help suppress such backgrounds.

- Due to the small center of mass energy, $\sqrt{s} \sim 4.5$ GeV, there are no backgrounds from B-meson decays.

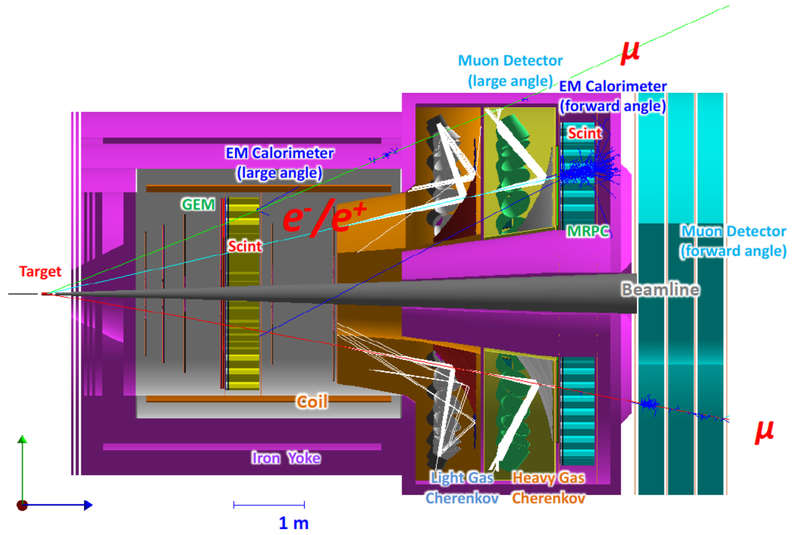

Fig. 3. The SoLID J/Ψ configuration with muon detectors [28]. Other sub-detectors are labeled.

More detailed simulation studies needed to estimate the impact of acceptance and backgrounds on CLFV limits.